ACS APPLIED MATERIALS & INTERFACES

Research Article

www.acsami.org

Hierarchically Structured ZnO/Petal Hybrid Composites with Tuned Optoelectronic and Mechanical Properties

Cheolmin Park,[†,‡] Hye-Mi So,[‡] Hyeon Jun Jeong,[§] Mun Seok Jeong,[§] Eckhard Pippel,[∥] Won Seok Chang,*[,†,‡] and Seung-Mo Lee*[,†,‡]

[†]Nano Mechatronics, Korea University of Science and Technology (UST), 217 Gajeong-ro, Yuseong-gu, Daejeon 305-333, South Korea

[‡]Department of Nanomechanics, Nano-Convergence Mechanical Systems Research Division, Korea Institute of Machinery & Materials (KIMM), 156 Gajungbuk-ro, Yuseong-gu, Daejeon 305-343, South Korea

[§]Department of Energy Science, Center for Integrated Nanostructure Physics, Institute for Basic Science, Sungkyunkwan University, 2066 Seobu-ro, Suwon 440-746, South Korea

[∥]Max Planck Institute of Microstructure Physics, Weinberg 2, D-06120 Halle (Saale), Germany

ABSTRACT: Impressive biophotonic functions of flora in Mother Nature are often attributed to the optical diffraction occurring on hierarchically structured surfaces. The petals, displaying vivid colors, have diverse surface structures. The shapes of those structures alter significantly depending on the part of the petal, and they adjust the intensity of the reflected color and the light absorbance. Here, we added semiconducting properties to those intriguing optical functions arising from the unique surface structures. By means of atomic layer deposition (ALD), we conformally deposited a ZnO layer on the yellow rose petal, which has hierarchical surface structures and exhibits peculiar light absorbance behaviors. The resulting ZnO/petal composites revealed unique optoelectronic characteristics by synergetic effects between the biophotonic structures and inherent semiconducting properties. From several control experiments, we identified that the biophotonic hierarchical structures give rise to strong modulation of the light absorbance. We found that ZnO/petal exhibits superior mechanical stability to the raw petal likely due to the Zn infiltration into the petal. The design inspired by floral creatures with photonic structures and manufactured in the form of composite with mechanical stability and distinctive optoelectronic properties is believed to offer a new paradigm for the preparation of bioinspired photonic devices.

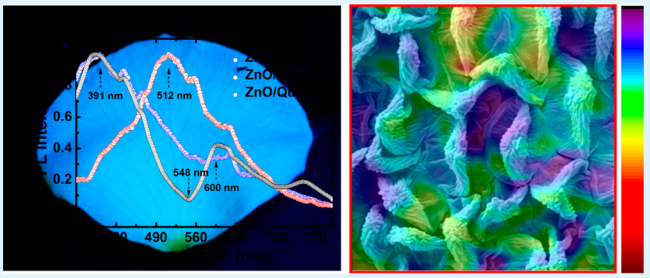

KEYWORDS: *biophotonic hierarchical structure, flower, zinc oxide, atomic layer deposition, biotemplate*

INTRODUCTION

The astonishing diversity of biological photonic structures present in Mother Nature today is the fruit of continuous evolution. Knowledge of such structures can surely provide a great inspiration for novel photonic applications. Biologically inspired design of photonic structures enables one to provide a nearly unlimited variety of specific templates for future optical technology.[1−3] The petals displaying vivid color, one of those biological structures, have ultraviolet (UV) patterns (high ultraviolet absorbance, i.e., a nectar guide) near the center, invisible to humans but visible to insects. The high absorbance of the petals depends strongly on the surface morphologies of the epidermal cells containing the pigments,[4,5] which are, in general, composed of special micropapillae covered with nanoridges, i.e., hierarchical structures. The presumable biological functions of such hierarchical structures were described nearly a century ago.[6] It has been reported that the structures attract insect pollinators by holding glistening dew drops (likely by petal effect)[7] or providing a tactile stimuli for surface recognition.[8] From the perspective of biological function and involved biophotonics, flowers have to effectively absorb sunlight in the region of visible as well as UV light to exhibit more attractive optical appearance to pollinators.[9] Naturally, the surface of the petals must have brilliant photonic structures ensuring the highest possible light absorption, i.e., light-trapping.[10,11] Thus, these hierarchical structures present in the petal could be adopted as a role model for the effective structure with negligible optical losses, which are greatly required in the field of photovoltaic applications. This lesson mining from nature inspired us to create a novel photonic device emulating structure-induced biophotonic features of petals.

To materialize such photovoltaic elements, the hierarchical structures of the petal have to be reproduced with complete fidelity on the surface of the man-made active materials with photovoltaic properties. Technically, however, this is not such

Received: July 8, 2014
Accepted: August 25, 2014
Published: August 25, 2014

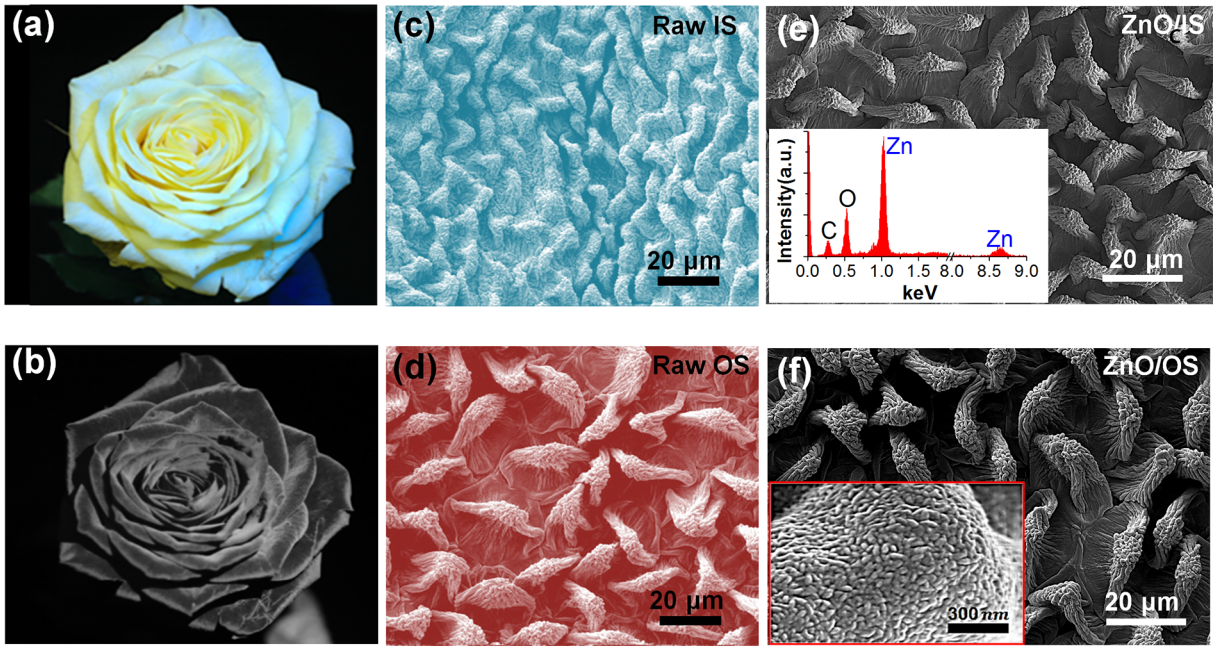

Figure 1. Characterizations and surface morphology of a raw yellow rose and a ZnO deposited petal. (a, b) Photograph of natural yellow rose in daylight and UV light, respectively. (c, d) SEM micrographs taken from proximal (inner side, raw IS) and distal regions (outer side, raw OS) in the dried petal, respectively. (e, f) SEM micrographs of inner side and outer side of ZnO deposited petal, respectively. The inset in (e) shows the EDX spectrum. The insert in (f) shows the ZnO grain.

an easy undertaking. Provided that conformality can be guaranteed, the replication approach could be the best possible solution. The resulting replica may also introduce some superlative properties induced by synergetic effects between the used biotemplates and the coated man-made materials (in particular, oxides),[12−14] so long as the conformal replication can be done and the as-coated film can have high crystallinity. In general, oxides require high processing temperatures to be crystallized. This implies that the resulting oxide/petal composites may be mechanically too fragile to be used for the intended applications. However, this issue can be readily resolved, if one uses the composites just as is without removing the petal, or if the employed oxide can be crystallized by low-temperature processing. Unlike other oxides requiring high processing temperatures to crystallize, ZnO with good crystallinity and extreme conformality can be coated on diverse biological templates by means of low-temperature atomic layer deposition (ALD) technique.[12−14] Here, through ZnO ALD, ZnO/petal composites with good mechanical stability were prepared. Interestingly, the native petals revealed peculiar location-dependent absorption characteristics due to the variations of hierarchical structures present on the petal. As compared to flat ZnO without any structural feature, ZnO coated on the petal, excluding any pigment effect of the petal, showed noticeable optical absorption enhancements in the UV as well as visible range in concert with the optical properties of the deposited ZnO. In addition, the photocurrent generated by ZnO exhibited distinct structure- and location-dependent trends as well. The design inspired by floral creatures and manufactured in the form of composite with mechanical durability and distinctive optoelectrical characteristics could herald a new paradigm for the preparation of bioinspired photonic devices.

EXPERIMENTAL SECTION

Preparation of a Dried Yellow Rose Petal. Individual rose petals were pulled out from living yellow roses that were purchased from a local flower garden in Daejeon, Korea. After being cleaned carefully with deionized water, a petal was sandwiched between two 5 × 5 cm^2 slide glasses and kept at room conditions for drying.

ZnO ALD. The rose petal was placed in an ALD reactor (Savannah 100, Cambridge Nanotech, Inc.) and dried at 70 °C for 30 min in vacuum (1×10^{-2} Torr) with a steady N_2 gas stream (20 sccm). For the ZnO deposition, DEZn (diethylzinc, $Zn(C_2H_5)_2$, Sigma-Aldrich) and deionized H_2O were used as zinc and oxygen sources, respectively. During the deposition process, the petals were alternately exposed to/purged from $Zn(C_2H_5)_2$ and H_2O vapor for 250 cycles. The pulse/exposure/purge time of $Zn(C_2H_5)_2$ and H_2O was 0.1/30/40 s and 0.1/30/40 s, respectively.

Characterizations. The absorbance of each sample was measured by UV−vis−NIR spectrophotometer (UV-3600, Shimadzu) in the spectral range of 350−800 nm with 0.5 nm resolution. The background noises of the sample were corrected by measuring the reference. The macrophotoluminescence (macro-PL) spectra of ZnO deposited samples were measured using a spectrofluorometer (FluoroLog-3) in the spectral range of 350−700 nm with 0.35 nm resolution. Its excitation light is 295 nm wavelengths, and the sample was positioned at 45 deg between the excitation light and the detector with a spot size of 1.5 × 1.5 cm^2. Spatially resolved micro-PL mapping was performed by NT-MDT, NTEGRA-SPECTRA, with a 355 nm wavelength of excitation. The scan area of 75 × 75 μm^2 was measured by a 40× objective lens with ∼800 nm spatial resolution. After osmium coating of 5 nm thickness on the samples, the morphology was carefully measured by field emission scanning electron microscope (FE-SEM, S-4800, Hitachi) of cold type with 1 kV acceleration voltage and 8.6 pA emissions current. The crystallinity of the deposited ZnO was measured by an X-ray diffractometer (XRD, Bruker D8 Advance) with Cu Kα radiation (wavelength λ = 1.5418 Å). The 2 theta range was from 20−80 deg with a scan speed of 0.2 deg/min. The determination of the chemical nature of the deposited ZnO on the petal was performed by an X-ray photoelectron spectrometer (XPS, KRATOS, AXIS NOVA). For the preparation of the cross-sectional samples of the ZnO/petal, a focused ion beam was used. Transmission

electron microscope (TEM) and energy-dispersive X-ray (EDX) investigations (imaging and point analyses) were performed with a FEI TITAN 80−300 microscope (300 kV) in scanning transmission mode. For photocurrent measurement, the Ti/Au electrode of 30/500 nm thickness was deposited on the surface of the ZnO/petal composites and ZnO/quartz by thermal evaporation method (KOREAVAC, KVE-T2000) with a shadow mask (gap = 50 μm). During the thermal evaporation process, the sample holder was water-cooled to avoid thermal damage to the ZnO/petal. In a dark room, the photogenerated currents of ZnO/petal and ZnO/quartz were measured using a high-speed source/monitor unit (E5262A, Agilent Technologies) with illumination of 355 nm laser (CNI, DOI-UV-F-355-CW, 11.5 mW/cm^2).

Tensile Test. All samples (2 mm × ∼3 cm) were carefully cut with a knife (BAYHA, Blades, No. 24) under the optical microscope (Leitz Aristomet); subsequently those were mounted in a thick paper jig (∼500 μm thick) having 20 mm punched holes. The paper jigs were used to enable alignment and clamping of the specimens during the tensile test. Furthermore, the jigs allowed the specimens to be cut easily through the cutting line so that specimen and paper jigs were not loaded together during the actual test. Pattex Blitz Kleber (Henkel, Germany) was used as glue to fix the sample to the edge of the jigs. A ZWICK 1445 tensile test machine with 500 g HBM load cell with 0.1 mN resolution and 0.5% uncertainty was used. The upper part of the jig was fixed to the load cell by a screw-type clamping system, and subsequently the jig was cut through the middle line with scissors. After controlling the vertical alignment of the specimen attached to the jig, the lower part of the jig was also fixed in the same way as the upper part. The extension rate was 10% of the initial length per minute (2 mm/min). The sample was extended until failure occurred. SEM and optical microscope were used to measure and confirm the cross-sectional area of the specimens. Because the thickness of the sample was not perfectly uniform, along the horizontal direction of each sample, at many points the thicknesses were measured and averaged. In the case of the width of each sample, a similar procedure was applied. On the basis of the measured cross-sectional area, the raw force (mN)−strain (%) data for each specimen exported from the software of the machine were rescaled into the engineering stress (σ)−strain (ε). To obtain a tensile testing curve of one sample, more than 15 samples were prepared identically and measured at identical conditions. All graphic works including data rescaling were performed with ORIGIN 8.0.

RESULTS AND DISCUSSION

In fauna, structural color, originating from physical interactions of light with photonic micro/nanostructures, has been reported in a range of animal species, while in flora, examples of photonic structures are quite rare. In addition, those have been very recently demonstrated.[9,15] Particularly, the color of the petal is believed to be changed with the chemical nature of the pigments. However, it is known that the intensity of the reflected color depends strongly on the shape and dimension of epidermal cells.[4] For instance, a yellow petal (Figure 1a) contains pigments that absorb green and blue light, allowing the yellow light to pass through and out of the petal.[16] Although the petal appears yellow to us, it can be figured out that there exists a nectar guide with strong absorption of UV light (Figure 1b). The strong UV absorption was believed to be induced by the differential distribution of flavonoids in some plants.[17] However, in the case of the yellow rose petal used in this research, the microstructure investigation by scanning electron microscope (SEM) indicated that the morphology and distribution of the hierarchical structures (nanoridges on micropapillae) on the petal vary with the location. Namely, though micropapillaes covered with nanoridges are widely spread in common in both the proximal region (inner side) and the distal region (outer side) of the petal, the sizes of individual micropapillae become smaller as the location gets closer to the inner side of the petal, as can be recognized from Figure 1c and d. It is known that the strong UV absorption likely results from hierarchical structures present on the petal and cannot be caused by pigments alone.[18] Taking into account the observation that the petal has a strong UV absorption region, the semiconducting ZnO having good optoelectronic properties was deposited on the petal by ALD processing at 70 °C. First, to validate the effect of the hierarchical structure on the optoelectronic properties of ZnO, a reference flat ZnO without surface structure (ZnO/quartz) was prepared on the flat quartz plate (with average roughness of 0.33 nm) under the same deposition conditions as the ZnO/petal replica. The deposited ZnO with a thickness of ∼50 nm on the petal revealed good conformality (Figure 1e and f) as well as crystallinity (Figure 2a). Although all samples showed crystalline phases, the

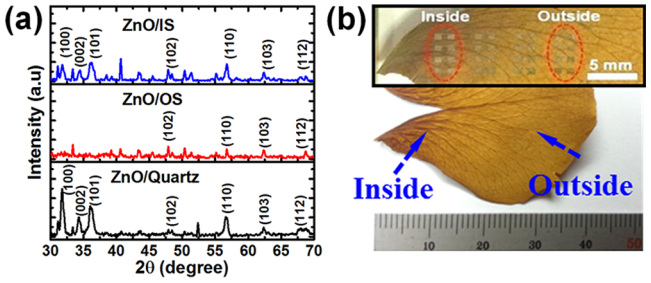

Figure 2. (a) Wide-angle X-ray diffraction (WAXD) spectra of the ZnO deposited on the petal and quartz. (b) ZnO deposited petal with electrodes for optoelectronic property characterization.

individual peak intensity of the ZnO deposited on inner-side petal (ZnO/IS) was measured to be lower than that of the flat ZnO/quartz. Furthermore, the ZnO deposited on the outer-side petal (ZnO/OS) did not show wurtzite phase. These differences in crystal growth are likely induced by the nanoscale morphology and resulting geometric constraint effect. To characterize optoelectronic properties of the resulting ZnO/petal composites, Ti/Au electrodes of 30/500 nm thickness were deposited on the composites (Figure 2b). Because the petal has different hierarchical surface structures depending on the location, the optical and electrical properties of the petal were greatly changed by the introduction of the thin semiconducting ZnO, as can be recognized from Figure 3.

While the pure quartz plate showed low absorbance in the UV region as well as the visible region, the ZnO/quartz showed characteristic absorbance in the UV region by the introduction of ZnO (Figure 3a). The petal samples revealed rather different trends. Although both the outer (raw OS) and inner sides (raw IS) of the petal showed considerably higher absolute absorbance through the whole wavelength range than the flat ZnO/quartz, in the UV region the outer side showed higher absorbance than the inner side. ZnO deposition led to a decrease in absorbance of the outer side over a whole range of wavelength. In contrast, the absorbance of the inner side of the petal was observed to increase in the UV range and decrease in the visible range by the introduction of the thin ZnO layer. An intersection of absorbance appeared around the 400 nm region. These distinct differences in absorbance were believed to be caused by surface structure rather than pigmentation. For elucidating the effect of the structure on the absorbance, the measured absorbance spectra were further processed. Namely, as can be seen in Figure 3b, the absorbance spectra of raw

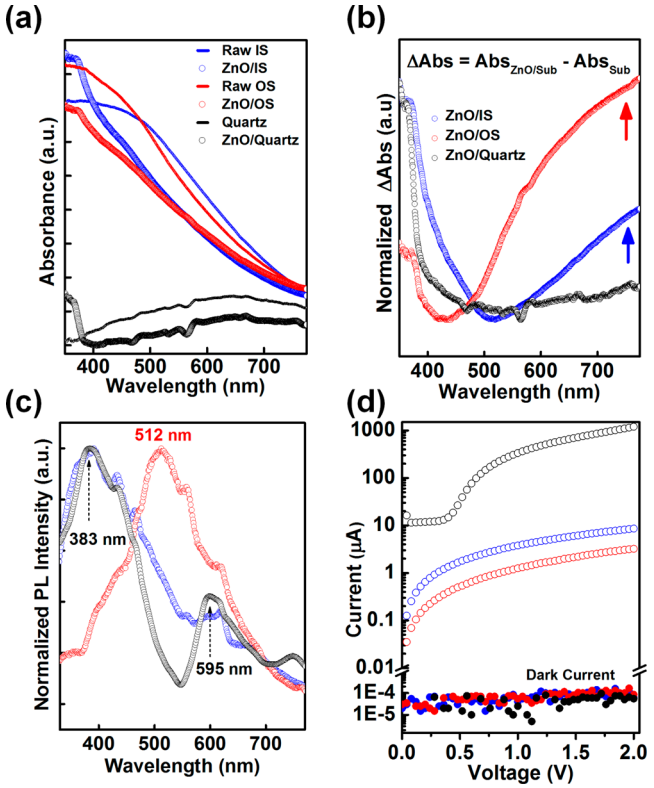

Figure 3. Optoelectronic properties of ZnO/petal composite. (a) Absorbance spectra of raw petals and diverse ZnO samples. The intensity is absolute value. (b) Absorbance spectra excluding pigmentation effect. See the details in the text. (c) Room-temperature PL spectra of ZnO/petal composites and flat ZnO deposited on quartz. The incident beam spot size was 1.5 × 1.5 cm^2. (d) *I*–*V* characteristics of photocurrents excited by 355 nm wavelength laser.

templates (substrates) were subtracted from spectra of templates with ZnO, and then each spectrum was normalized. The flat ZnO film ($E_{g,ZnO}$ = 3.37 eV at room temperature) shows typical absorbance features of semiconducting material with a wide band gap: strong/negligible absorbance below/above ~375 nm wavelength, respectively.[19] By contrast, the hierarchically structured ZnO revealed peculiar absorbance characteristics led by the semiconducting effect of ZnO itself as well as the structural effect. While ZnO/OS showed low UV absorbance and high visible absorbance, ZnO/IS showed high UV absorbance and low visible absorbance. This spectral feature was believed to be caused by the differences in hierarchical structures between the inner side and the outer side of the petal. Our supposition was further clarified by the room-temperature photoluminescence (PL) measurement. As can be recognized from Figure 3c, the flat sample (ZnO/quartz) exhibited typical PL features of ALD-grown ZnO, i.e., near-band-edge (NBE) UV emission around 383 nm and green band emission around 595 nm. The ZnO/IS showed broadening of NBE and green band emission. In contrast, the ZnO/OS showed relatively large green band emission. It is well-known that the PL of ZnO has a strong dependence on the morphology. Particularly, the intensity of the green band emission was reported to be proportional to the area-to-volume ratio.[20] As can be seen in Figure 1c and d, the outer-side petal has larger and deeper feature size than the inner-side petal, which implies that the outer side has larger area-to-volume ratio than the inner side. The PL and absorbance indicates that the replicated hierarchical structures from the petal have a great influence on the optical properties of ZnO. Because of these differences in the optical properties induced by the structure, the ZnO/petal composites understandably exhibited distinct optoelectronic properties (Figure 3d). The photocurrent was measured under the illumination of 355 nm laser with sweeping bias voltage. Corresponding to the PL data, photoconduction behaviors were observed. ZnO/IS has higher value than ZnO/OS under UV illumination. Considering the complicated carrier path caused by hierarchical structures, the magnitudes of differences in the photocurrent of each sample were trivial.

So far, we demonstrated that the surface of the yellow rose petal has hierarchically structured biophotonic structures differing from location to location on the same petal. ZnO deposition on the petals was observed to create a synergy effect. Namely, the resulting ZnO/petal composites took on the character of a new creature having both optoelectronic properties of ZnO and biophotonic properties of the petal. As mentioned, the petal surface has variations of the biophotonic structures with location and an optimized morphology enabling the light-trapping effect.[10,11] To validate these issues, we further investigated the surface of the ZnO/petal composite by means of micro-PL mapping. As already described, the sizes of the individual epidermal cells on the petal become smaller and smaller toward the base (inner side). Finally, at the base of the petal, micropapillae were only rarely able to be found and only nanosized wavy striations existed as shown in Figure 4a. Comparing the micro-PL mapping image

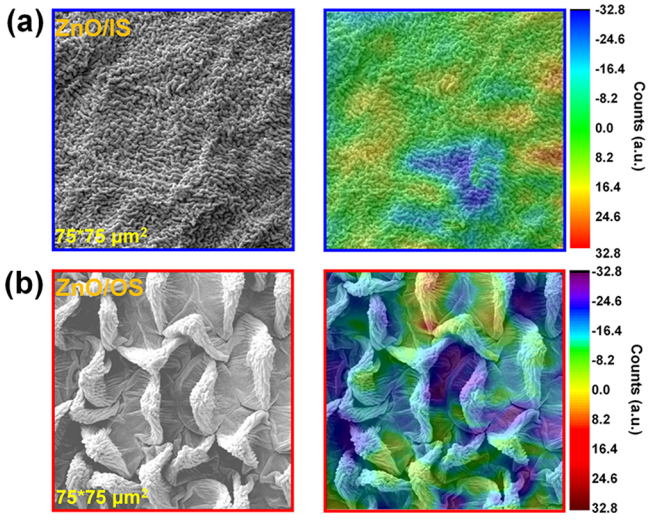

Figure 4. Microphotoluminescence (micro-PL) mapping images in a range of 360–420 nm wavelength with spatial resolution of 800 nm. Images in the left column are SEM micrographs of the base part (a) and the outer-side part (b) of the petal, respectively. Images in the right column are micro-PL mapping images overlapped on SEM micrographs in the left-hand side, respectively.

of 360–420 nm wavelength range measured from the base (Figure 4a) and the outer side (Figure 4b) of the ZnO deposited petal, the PL intensity from the base part is shown to be in general much stronger than the intensity from the outer-side part. It is thought that the complex nanosized wavy structure induces the light-trapping effect, which leads to relatively higher PL emission on the base than the outer side. Another noteworthy observation was that the PL intensities of UV on both samples are less uniform than expected, in

particular, the outer side of the petal. As can be noticed from the PL mapping image in Figure 4b, the PL intensity in valleys between micropapillaes is generally weaker than it is on the top of the micropapillaes. Currently those different intensity distributions are presumed to be caused by the light-trapping effect of the hierarchical structures because the micropapillaes covered with nanoridges have more effective light trapping than the valley area with a flat surface.[10,11] Because we used dried rose petals, the shrinkage of the epidermal cells was inevitable. Once the shape of the epidermal cell can be preserved without shrinkage during drying, the light-trapping effect is likely maximized and, consequently, the PL intensity of the ZnO/petal could be significantly enhanced.

No matter how good the performance of any optical device is, it can never be used unless the device is mechanically stable. Therefore, the mechanical stability is the most pressing matter to be taken care of, although it always takes second place to other physical properties in most scientific communities. Our ZnO/petal composites showed intriguing optoelectronic behavior led by combined effects of the ALD-grown ZnO with semiconducting functions and the petal with biophotonic functions. In previous reports, it was demonstrated that application of ALD to certain biological material could bring about unanticipated improvement of mechanical properties due to the infiltration effect of the transition metals that are used for metal source precursors.[12−14] In this research, as can be seen in Figure 5a, a similar phenomenon was observed that was not

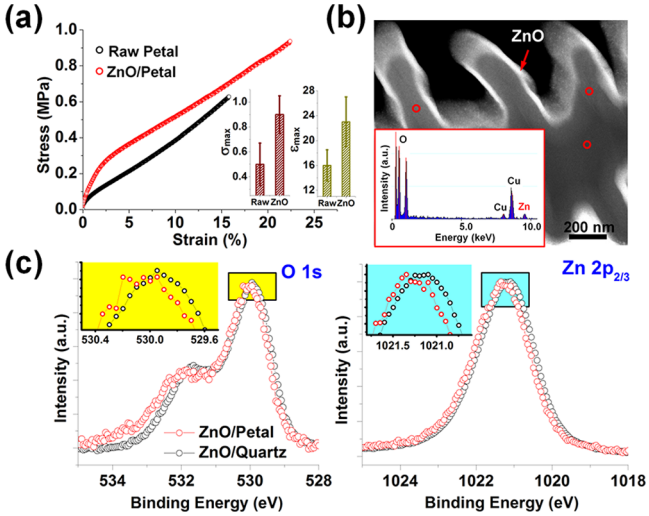

Figure 5. Mechanical stability of ZnO/petal composites. (a) Representative uniaxial tensile testing curves of the raw dried petal and the ZnO deposited petal, respectively. The inset shows comparison of failure stress and failure strain of both samples. (b) TEM image. The red circles indicate the locations where EDX element analysis was carried out. The inset shows a representative EDX element analysis result. (c) XPS measurement results. The left and right images show the shift of the O 1s and Zn 2p core-level, respectively. The inset in each figure is a magnified image of the yellow or the cyan colored region, respectively.

expected. Normally, the dried petal is much more brittle as compared to the nondried petal. However, ZnO/petal shows slightly increased failure strength as well as failure strain in comparison to the raw dried petal. It was found that a tiny amount of Zn is infiltrated into the inner structure of the petal (Figure 5b). The involved mechanism leading to such an increase is not clear as of now. However, as can be recognized from X-ray photoelectron spectroscopy (XPS) measurement results (Figure 5c), the infiltrated Zn appeared to form additional bonds to any other element inside the petal. The shifts of the Zn 2p and O 1s core levels also could be attributed to the differences in morphologies.[21] The observed shift is believed to be due to Zn-meditated additional chemical bonds though, taking into account that the core level shifts by morphological differences tend to be much larger.[21,22]

CONCLUSIONS

In summary, the incorporation of semiconducting ZnO into the unique hierarchical biophotonic structures of the petal produced a novel composite that reveals the synergistically combined properties of man-made materials and natural materials. The ZnO/petal hybrid composites exhibited intriguingly tuned characteristics of light absorbance as well as photoluminescence, as well as impressive optoelectronic property. Additionally, by virtue of the low-temperature processability of ZnO ALD, the mechanical stability of the ZnO/petal composites was able to be preserved and even enhanced, likely by the infiltration of tiny amounts of Zn into the petal. Because potential biotemplates with peculiar optical functions directly usable for a device abound in Mother Nature, our report could open new possibilities for the preparation of a wide range of bioinspired synthetic composites with varying optoelectronic and mechanical properties.

AUTHOR INFORMATION

Corresponding Authors

*W. S. Chang e-mail: paul@kimm.re.kr.
*S.-M. Lee e-mail: sm.lee@kimm.re.kr.

Notes

The authors declare no competing financial interest.

ACKNOWLEDGMENTS

S.-M.L. greatly acknowledges financial support by the Research Programs (KM3220 and SC 0970) funded by of Korea Institute of Machinery and Materials (KIMM). W.S.C. acknowledges financial support by the Global Frontier R&D Program by the Center for Advanced Soft Electronics funded by the National Research Foundation under the Ministry of Science, ICT and Future Planning (2013M3A6A5073183), and the Basic Research Fund from KIMM.

REFERENCES

(1) Vukusic, P.; Sambles, J. R. Photonic Structures in Biology. *Nature* **2003**, *424*, 852−855.
(2) Lee, L. P.; Szema, R. Inspirations from Biological Optics for Advanced Photonic Systems. *Science* **2005**, *310*, 1148−1150.
(3) Parker, A. R.; Townley, H. E. Biomimetics of Photonic Nanostructures. *Nat. Nanotechnol.* **2007**, *2*, 347−353.
(4) Kay, Q.; Daoud, H.; Stirton, C. Pigment Distribution, Light Reflection and Cell Structure in Petals. *Bot. J. Linn. Soc.* **1981**, *83*, 57−83.
(5) Vignolini, S.; Moyroud, E.; Glover, B. J.; Steiner, U. Analysing Photonic Structures in Plants. *J. R. Soc. Interface* **2013**, *10*, 20130394.
(6) Martens, P. Origine et Rôle des Plissements Superficiels sur L'épiderme des Pétales Floraux. *C. R. Acad. Se. Paris* **1933**, *197*, 785−787.
(7) Feng, L.; Zhang, Y.; Xi, J.; Zhu, Y.; Wang, N.; Xia, F.; Jiang, L. Petal Effect: A Superhydrophobic State with High Adhesive Force. *Langmuir* **2008**, *24*, 4114−4119.

(8) Koch, K.; Bhushan, B.; Barthlott, W. Diversity of Structure, Morphology and Wetting of Plant Surfaces. *Soft Matter* **2008**, *4*, 1943−1963.
(9) Whitney, H. M.; Kolle, M.; Andrew, P.; Chittka, L.; Steiner, U.; Glover, B. J. Floral Iridescence, Produced by Diffractive Optics, Acts as a Cue for Animal Pollinators. *Science* **2009**, *323*, 130−133.
(10) Exner, F.; Exner, S. Die Physikalischen Grundlagen der Blütenfärbungen. *Sitzungsber. Kais. Akad. Wiss. Wien, Math.-nat. Kl. I* **1910**, *119*, 191−245.
(11) Bernhard, C. G.; Gemne, G.; Moller, A. R. Modification of Specular Reflexion and Light Transmission by Biological Surface Structures. *Q. Rev. Biophys.* **1968**, *1*, 89−105.
(12) Lee, S. M.; Pippel, E.; Gösele, U.; Dresbach, C.; Qin, Y.; Chandran, C. V.; Bräuniger, T.; Hause, G.; Knez, M. Greatly Increased Toughness of Infiltrated Spider Silk. *Science* **2009**, *324*, 488−492.
(13) Lee, S. M.; Grass, G.; Kim, G. M.; Dresbach, C.; Zhang, L.; Gösele, U.; Knez, M. Low-Temperature ZnO Atomic Layer Deposition on Biotemplates: Flexible Photocatalytic ZnO Structures from Eggshell Membranes. *Phys. Chem. Chem. Phys.* **2009**, *11*, 3608−3614.
(14) Lee, S. M.; Pippel, E.; Moutanabbir, O.; Gunkel, I.; Thurn-Albrecht, T.; Knez, M. Improved Mechanical Stability of Dried Collagen Membrane after Metal Infiltration. *ACS Appl. Mater. Interfaces* **2010**, *2*, 2436−2441.
(15) Lee, S. M.; Üpping, J.; Bielawny, A.; Knez, M. Structure-Based Color of Natural Petals Discriminated by Polymer Replication. *ACS Appl. Mater. Interfaces* **2011**, *3*, 30−34.
(16) Glover, B. J. *Understanding Flowers and Flowering: An Integrated Approach*; Oxford University Press: Oxford, U.K., 2007.
(17) Rieseberg, L. H.; Schilling, E. E. Floral Flavonoids and Ultraviolet Patterns in Viguiera (Compositae). *Am. J. Bot.* **1985**, *72*, 999−1004.
(18) Whitney, H. M.; Kolle, M.; Alvarez-Fernandez, R.; Steiner, U.; Glover, B. J. Contributions of Iridescence to Floral Patterning. *Commun. Integr. Biol.* **2009**, *2*, 230−232.
(19) Luka, G.; Krajewski, T.; Wachnicki, L.; Witkowski, B.; Lusakowska, E.; Paszkowicz, W.; Guziewicz, E.; Godlewski, M. Transparent and Conductive Undoped Zinc Oxide Thin Films Grown by Atomic Layer Deposition. *Phys. Status Solidi A* **2010**, *207*, 1568−1571.
(20) Andelman, T.; Gong, Y.; Polking, M.; Yin, M.; Kuskovsky, I.; Neumark, G.; O'Brien, S. Morphological Control and Photoluminescence of Zinc Oxide Nanocrystals. *J. Phys. Chem. B* **2005**, *109*, 14314−14318.
(21) Al-Gaashani, R.; Radiman, S.; Daud, A. R.; Tabet, N.; Al-Douri, Y. XPS and Optical Studies of Different Morphologies of ZnO Nanostructures Prepared by Microwave Methods. *Ceram. Int.* **2013**, *39*, 2283−2292.
(22) Zhou, H.; Li, Z. Synthesis of Nanowires, Nanorods and Nanoparticles of ZnO through Modulating the Ratio of Water to Methanol by Using a Mild and Simple Solution Method. *Mater. Chem. Phys.* **2005**, *89*, 326−331.